Proceedings of the 3rd
RSI International Conference on Robotics and Mechatronics
October 7-9, 2015, Tehran, Iran

The Analysis and Simulation of a Tethered Segway

Mohammad Hossein Salehpour
Control and Intelligent Processing Center of Excellence
School of Electrical Engineering
University of Tehran
Tehran, Iran
m.h.salehpour@ut.ac.ir

Hadi Moradi
Control and Intelligent Processing Center of Excellence
School of Electrical Engineering
University of Tehran
Tehran, Iran
Intelligent Systems Research Institute, SKKU, South Korea
moradih@ut.ac.ir

***Abstract*— In this paper we present the design and analysis of a tethered Segway designed for moving over steep surfaces such as dome shaped structures. This robotic platform, inspired from human climbers who use a cable to keep themselves stable on steep surfaces, consists of a simple Segway and a mechanism used to tether the robot to the top of the surface. The mathematical model of the robot is derived using Lagrangian approach and the control is developed based on a state feedback gain. The model consists of a two wheeled inverted pendulum driven by two DC motors. Also there is a DC motor used to control the length of the cable tethering the robot to the top. The control inputs are the voltages applied to each DC motor. The system has been simulated and the results show that the controller can move the robot around while keeping its stability on steep surfaces up to 75 degrees.**

Keywords— tethered robot, robotic platform, stabilization, model of Segway, Lagrangian approach, state feedback

I. INTRODUCTION

The invention of Segway introduced a new way of moving around on two wheels based on a sophisticated control system. There have been a lot of research on using different controllers to control a Segway better. Despite the novelty of the Segway's design, it cannot stably move on steep surfaces due to lack of enough friction force to keep the robot stable on such a surface. An example of such surfaces are domes that are one of the attractive structures in many ancient architectures, which need to be inspected, cleaned, and repaired (Fig. 1). Since these surfaces, are not easily reachable, due to their unique design and steep surface, it is hard and dangerous to climb domes especially those with high slops which climbing them needs expertise and experience.

Based on the safety issues and high demand for autonomous systems, using robots to perform service tasks in such dangerous situations is an interesting research both from theoretical and practical point of view. There have been attempts to design and develop robot climber to climb walls and steep surfaces [4, 5, and 6]. However, these are not suitable for domes due to their dependence to the surface condition. In a recent research a multi robot platform was designed and simulated that can stably move all over a dome. The multi-robot platform consists of a leader and supporter robot(s) to provide stability for the whole system [1, 2]. Despite the novel design of this multi-robot system, its complexity has been an issue.

This project is partially supported by the Hosseinieh-Ershad foundation

Fig. 1 (a) A dome in Isfahan, Iran. Steep surfaces on domes are hardly accessible.

Consequently, a single tethered robot had been designed implemented and tested successfully for dome inspection, repair, and maintenance (**Error! Reference source not found.**(a)) [3]. In this design, the robot can be installed once on top of a dome, in a dedicated housing, and perform the tasks whenever needed. The "Dome Tethered Robot" has a simple design, based on a differential–drive locomotion mobile robot attached to top of domes. The implemented robot consists of a tether mechanism so that it can control the tether's length while operating on a dome [3]. The "Dome Tethered Robot" design had been inspired from human dome climbers using a rope to keep themselves stable on a dome.

In this paper we have reported the controller design for the tethered dome robot which is actually a tethered Segway.

II. RELATED WORKS

There are many robotic methods for climbing steep surfaces and walls including magnetic systems [4], systems with adhesive materials [5], suction and vortex [6]. These methods are note suitable for dome climbing due to rough and dirty surface of domes with cracks, especially if they are made of materials like clay, brick, and ceramic. Furthermore, these methods normally need electric power for stability which makes them prone to failure in case of power failure. Obviously the magnetic-based mechanism are not suitable for domes.

978-1-4673-7234-3/15/$31.00 ©2015 IEEE

(a)

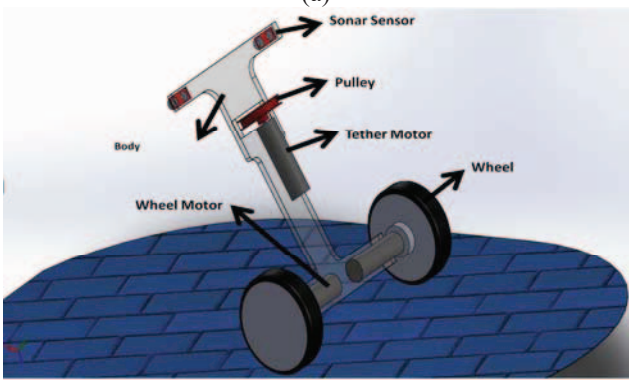

(b)

Fig. 3 (a) The implemented tethered Segway on a dome (b) Tethered Segway schematics with a motor controlling the length of the tethered

To overcome the disadvantages involved in the aforementioned methods, a multi robot platform for climbing domes was designed [1, 2]. Beside this multi-robot system, a tethered robot has been designed, implemented, and tested which is a single-robot tethered robotic mechanism, inspired from human climbers [3]. The advantages of the tethered Segway is its faster and smoother movement compared to the multi-robot system or the other systems. Furthermore, this design is lighter compared to similar robotic systems which is an important factor to avoid damaging domes which are highly sensitive and vulnerable.

Controlling a Segway movements is an interesting field for researchers. The main goal of the classical Segway problem is to maintain stability by applying a suitable amount of torque to its wheels. This problem has been discussed using different approaches like modeling with Newton-Euler method or with Lagrangian function and controlling with a PID compensator or using state-feedback law [7, 8, 9]. However, to the best of our knowledge, there not been any study to address a tethered Segway.

In this paper we model a tethered Segway and design a controller to stably move it over a steep surface such as a dome. Here we are going to specify the desired platform mathematically model it using Lagrangian function method and control its movements not only with purpose of stability but also for tracking a desired set-point.

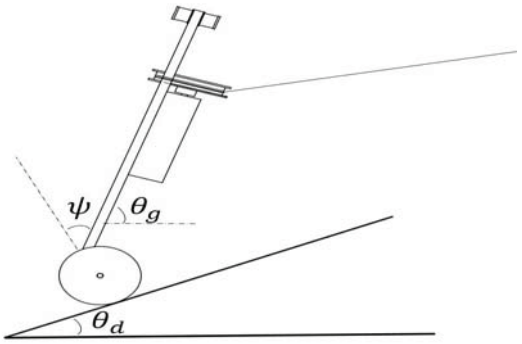

Fig. 2 Simple sketch of the tethered Segway robotic platform. $\theta_d, \theta_g, and\ \psi$ respectively indicate surface's slope in the operating point, robot's slope relative to the gravity vector, and robot's body pitch angle.

III. The Tethered Segway

The tethered Segway is a simple idea for moving on steep surfaces at high speed and low cost. It is a simple Segway which is equipped with a simple tethering mechanism that can be controlled to move stably on steep surfaces.

A. System Definition and Specification

The designed platform can be considered as a two wheeled inverted pendulum with a DC motor placed on the chassis coupled to a pulley that can control the length of the rope tethering the robot to the top of the steep surface (**Error! Reference source not found.** (b)). The two wheels are actuated using two DC motors, similar to a typical Segway. (**Error! Reference source not found.**(a)) shows an actual implementation of the tethered Segway, with slight differences and safety mechanisms, on a dome.

The robot is equipped with three rotary encoders that used to measure angular position and velocity of the wheels and the tether's pulley. Ultrasonic sensors are used to measure robot's body pitch angle which is one of the control variables beside wheels position and velocity. In addition to knowing Segway's pitch angle, a tilt sensor is used to measure the Segway's tilt is needed to indicate the surface's slope.

B. The Mathematical Model

As described above the system can be modeled as a two wheeled inverted pendulum with a tether mechanism. A simplified sketch of the robot as a simple two-wheeled robot is shown in (Fig. 2) with parameters exactly shown in the figure. The notations representing the system parameters are listed in Table I.

In this section we use the Lagrangian approach to derive mathematical model of the described system [10]. Considering the forces applied to the tether's pulley and the wheels coupled to the DC motors as an external force applied to the system we develop the dynamic equations of the system. Using basic equations for DC motors we can simply model the torque applied to the system by DC motors as a function of input voltages. So we aim to model the robotic platform with a

mathematical model which its outputs are robot's body pitch angle, body yaw angle, and its wheels angular position. To derive motion equations of the tethered Segway we assume that the direction of two-wheeled Segway is x-axis positive direction at $t = 0$. Each coordinate is given as following:

Table I The notations used in the modeling

	Unit	Description
θ_d	$[rad]$	Surface's slope at the operating point
θ	$[rad]$	Average angular position of the left and right wheel
ϕ	$[rad]$	The robot's body yaw angle
ψ	$[rad]$	The robot's body pitch angle
θ_g	$[rad]$	The robot's slope relative to the gravity vector, $\vec{g}$
θ_t	$[rad]$	The tether's angle relative to y-axis
θ_p	$[rad]$	The tether's angle relative to xy-plane
$T_{r,l,t}$	$[M.m]$	Torque supplied by the left, right, and tether motors
L	$[m]$	Body length
w	$[m]$	Body width
D	$[m]$	Body depth
h	$[m]$	Tether mechanism height
M_b	$[kg]$	Body mass
R	$[m]$	Wheel radius
Mw	$[kg]$	Wheel weight
Rt	[m]	Pulley's radius

$$\theta = \frac{1}{2}(\theta_l + \theta_r) \tag{1}$$

$$\phi = \frac{R}{w}(\theta_r - \theta_l) \tag{2}$$

$$m(x_m, y_m, z_m) = \left(\int R\dot{\theta}\cos\phi, \int R\dot{\theta}\sin\phi,\ R - R\theta\sin\theta_d\right) \tag{3}$$

Here $m(x_m, y_m, z_m)$ is central point of the wheel's axis, $\theta_{r,l}$ is wheel position (note that *r,l* indicate left and right). A brief look at (**Error! Reference source not found.**) shows that:

$$r(x_r, y_r, z_r) = \left(x_m + \frac{w}{2}\sin\phi, y_m - \frac{w}{2}\cos\phi, z_m\right) \tag{4}$$

$$l(x_l, y_l, z_l) = \left(x_m - \frac{w}{2}\sin\phi, y_m + \frac{w}{2}\cos\phi, z_m\right) \tag{5}$$

$$b(x_b, y_b, z_b) = \left(x_m + \frac{L}{2}\cos\phi\sin\psi, y_m + \frac{L}{2}\sin\phi\sin\psi, z_m + \frac{L}{2}\cos\psi\right) \tag{6}$$

in which *r, l, and b* indicate the right wheel's central point, the left wheel's central point, and the body's center of the mass, respectively. It is assumed that the tether mechanism is designed such that the mass is uniformly distributed and the tether mechanism and the chassis form a rigid body.

To calculate the Lagrangian function we need to calculate the translational kinetic energy E_t, the rotational kinetic energy E_r, and the potential energy U for the whole system. So we need to calculate inertia moment for different possible rotations in the

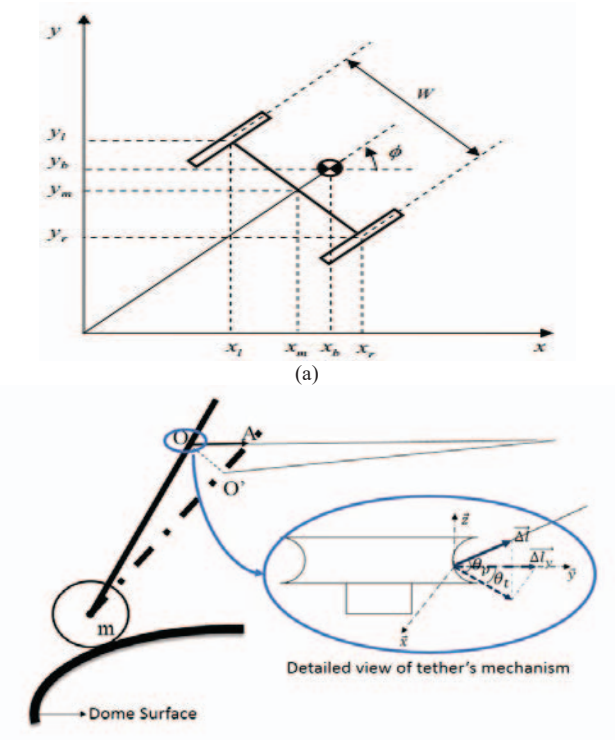

Fig. 4 (a) Wheels axis view in x-y plane (b) a simple sketch of the side view of the robot and the tether mechanism in more details. Note that we assume that the body pitch angle deviation small enough.

described system to calculate E_r as follows:

$$J_w = \frac{1}{2}M_w.R_w^2 \tag{7}$$

$$J_m = \frac{1}{3}M_m L_m^2 + \frac{1}{4}M_m R_m^2 \tag{8}$$

$$J_\psi = \frac{1}{12}M_b L^2 \tag{9}$$

$$J_\phi = \frac{1}{12}M_b\left(D^2 + w^2\right) \tag{10}$$

in which J_w, J_m, J_ψ, and J_{phi} are the inertia moment for wheels, inertia moment of the tether's DC motor, body pitch inertia moment, and body yaw inertia moment, respectively.

The translational kinetic energy E_t, the rotational kinetic energy E_r, and the potential energy U are:

$$E_t = \sum\left(\frac{1}{2}M_k v_k^2\right) \tag{11}$$

$$E_t = \sum\left(\frac{1}{2}J_k \omega_k^2\right) \tag{12}$$

$$E_t = \sum\left(M_k g_k Z_k\right) \tag{13}$$

in which v_k and ω_k are translational and rotational velocity of element k.

The Lagrangian function L is derived and using its

derivatives we can calculate the applied force in the coordinate system's directions.

$$\frac{d}{dt}\left(\frac{\partial L}{\partial \dot{q}}\right)-\frac{\partial L}{\partial q}=F_q \tag{14}$$

where q is a generalized coordinate and F_q is the torque applied to the system in its direction.

Note that the right-hand-side term can be calculated. These torques applied to the system i.e. the right-hand-side terms in (14), meet this set of equations:

$$\left(F_\theta,F_\phi,F_\psi\right)=\left(\frac{1}{2}\left(T_r+T_l\right),\frac{R}{w}\left(T_r-T_l\right),T_r+T_l-T_{ty}\right) \tag{15}$$

where $T_{r.l}\ and\ T_{ty}$ respectively represent torque of right and left wheels and torque applied as the cause of rope's tension.

Here we present a simple approach to derive the equation relating the operational torque T and the voltage applied to every DC motor's terminal V_t. These two basic equations are valid for all DC motors.

$$L_m I_a = V_t - K_b\dot{\theta}_m - R_m I_a \tag{16}$$

$$T = nK_t I_a \tag{17}$$

In equations above $R_m,\ K_b, n, and\ K_t$ are respectively the DC motor resistance, back EMF constant, gear ratio, and torque constant. Considering the motor inductance is negligible and is approximated as zero in (16), a DC motor's rotor current, I_a is:

$$I_a = \frac{V_t - K_b\dot{\theta}_m}{R_m} \tag{18}$$

Substituting I_a form (18) in (17) the operational torque can be calculated as:

$$T = \frac{nK_t}{R_m}\left(V_t - K_b\dot{\theta}_m\right) \tag{19}$$

where θ_m is the DC motor's rotor position. For more information about equations for DC motors, see [11].

To use this equation in the modeled tethered Segway system, we need to find each motor's rotor position. For the DC motors driving the robots wheels we can simply find out that:

$$\theta_{mr,ml} = \theta_{r,l} + \psi \tag{20}$$

in which $\theta_{mr,ml}\ and\ \theta_{r,l}$ are respectively the right and left motor's rotor position and right and left wheel's position. Also we need to find out the tether motor's rotor position, θ_{mu} to calculate the T_{ty} in equation (15). In (**Error! Reference source not found.**) a simple sketch of the tether mechanism is represented. What follows is a set of equations letting us to model the rope's length deviation:

$$\Delta l_y = \Delta l.\cos\theta_p\cos\theta_t \tag{21}$$

$$T_{ty} = \mathrm{T_t}.\cos\theta_p\cos\theta_t \tag{22}$$

Assuming that Δl is small enough in the triangle $OO'A$: $OO' \approx OA \approx \Delta L$. Hence we can find out that:

$$\frac{\Delta l_y}{h} = \tan\dot{\psi} \tag{23}$$

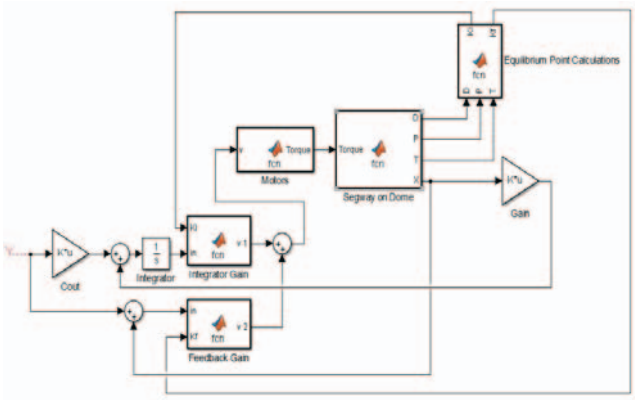

Fig. 5 The block diagram of the closed-loop system for the compensated system. The Controller Updater block updates the gain vectors periodically based on the programmed frequency.

where h is tether mechanism's height and for small Δl (23) can be approximated to:

$$\frac{\Delta l_y}{h} = \tan\dot{\psi} \approx \dot{\psi} \tag{24}$$

On the other hand assuming radius of the pulley as Rt we know that:

$$\Delta l = R_t.\dot{\theta}_{mu} \tag{25}$$

where $\dot{\theta}_{mu}$ is tether motor's angular velocity. Using (21), (23), and (25) we can derive the equation of $\dot{\theta}_{mu}$ as bellow:

$$\dot{\theta}_{mu} = \frac{h\dot{\psi}}{Rt.\cos\theta_p.\cos\theta_t} \tag{26}$$

Now combination of (19), (22), and (26) lead us to the following equation:

$$T_{ty} = \frac{nK_t}{R_m}\left(v_t - K_b\left(\frac{h\dot{\psi}}{Rt.\cos\theta_p.\cos\theta_t}\right)\right)\cos\theta_p\cos\theta_t \tag{27}$$

Now we can find an explicit solution for $\ddot{\theta}, \ddot{\phi}, and\ \ddot{\psi}$ solving the set of 3 equations obtained by substituting q with $\theta, \phi, and\ \psi$ in (14). Defining state variables, $x\ as\ x = \left[\theta, \dot{\theta}, \phi, \dot{\phi}, \psi, \dot{\psi}\right]^T$ and the input as $u = [v_r, v_l, v_t]^T$ will lead us to a state space representation of the tethered Segway as bellow:

$$\dot{x} = F\left(x,u\right) \tag{28}$$

$$y = x \tag{29}$$

C. *Variable Measurement*

In the previous section we modeled the tethered Segway system as a non-linear state space representation defined in (28) consisting of three non-state variables, $\theta_d, \theta_p, and\ \theta_t$. These variables are sensed at each time instance with proper sensors. Also state variables need to be sensed so that we can use the measured values as a feedback in the closed-loop system. We can calculate the surface's slope by subtracting the robot's body pitch angle from the body angle based on gravity vector measured by the tilt sensor on the robot. Note that, the Segway's body pitch angle can be measured by distance of a fixed point on robot to the ground.

D. Controller Design

It is easy to imagine that the system is not naturally stable. Our goal is to control the robot to move stably and smoothly on a steep surface and track the desired value assigned to each output using modern control theory. We have to move the robot in the same direction of the body pitch angle to keep it balanced and stable. Now that we have a mathematical model of the desired system as a MIMO system, we can control the robot for our desired response using modern control theory techniques, such as the state feedback method.

Although the classical Segway control problem focuses on regulating the robot's vertical angle, while changing the Segway's body pitch angle can have a great effect on providing the stability condition, e.g. leaning back while going down the steep surface, we aim on controlling the system in a way that it can track a desired value for variable ψ.

The system's block diagram is shown in Fig. 5. We have controlled the system with aid of the state feedback method. The inner loop, with gain K_f, is designed to stabilize the system and the outer one, with gain K_i, with integrator after the error signal is designed to provide the tracking. The integrator in the closed loop eliminates the error between output and the reference input [12].

This control policy is inspired by gain scheduling method where we linearize the model in different equili brium points and use the linearized model to calculate the feedback gain for the controller. This controller would be valid in an absorption area. So the robot have to choose how to behave and which controller to use based on in which absorption area its state is [13].

In order to control the system in a specific equilibrium point we have to linearize the system's model defined in (28). Given a specific equilibrium point, x_{ss} solving the equation below leads us to obtain input vector's value, u_{ss} in the stable operating point.

$$\dot{x}_{ss} = 0 \tag{30}$$

Solving the equation above yields an explicit answer for u_{ss}. Now we have to linearize the model in the operating point (x_{ss}, u_{ss}), so that:

$$\dot{x} = F(x,u) = F(x_{ss},u_{ss}) + A(x - x_{ss}) + B(u - u_{ss}) \tag{31}$$

$$y = x \tag{32}$$

where A *and* B denote the Jacobian of $F(x,u)$ evaluated at (x_{ss}, u_{ss}), given by:

$$A = J_x(x_{ss},u_{ss}) \tag{33}$$

$$B = J_u(x_{ss},u_{ss}) \tag{34}$$

In the above equation $J_x(x,u)$ represents Jacobian of F based on the state vector, x.

The state feedback controller is designed based on the linear model and the values of the non-state variables. In the block diagram shown in (Fig. 5) K_i and K_f are obtained using LQR method for closed-loop system that provides both stability and tracking. This controller is used in the closed-loop system so that the robot would behave as desired.

In our policy we use sensors to measure the value for non-state variables, i.e. $\theta_d, \theta_p, and\ \theta_t$, so we can use them to calculate the feedback gain. As these variables vary during the robot's movement on the steep surface we need to update our feedback gains periodically. Note that $\theta_p\ and\ \theta_t$ vary in a range of about $\frac{\pi}{4}$ radian during the motion on the steep surface and assuming that the slope, i.e. θ_d, changes at low rate, compared to the robot's speed, so we can use a lower update frequency.

E. Simulation results and discussion

The following values are considered to simulate the robot.

Table II Values assigned to the parameters for simulation

Parameter	Value	Unit	Description
g	9.81	$[\frac{m}{sec^2}]$	Gravity acceleration
L	0.4	$[m]$	Body length
w	0.3	$[m]$	Body width
D	0.01	$[m]$	Body depth
h	0.3	$[m]$	Tether height
M_b	1	$[kg]$	Body mass
R	0.04	$[m]$	Wheel radius
Mw	0.03	$[kg]$	Wheel weight
Rt	0.04	[m]	Pulley radius
L_m	0.12	[m]	DC motor length
M_m	0.2	$[kg]$	DC motor weight
R_m	6.69	[Ω]	DC motor resistance
K_b	0.468	$[\frac{V.sec}{rad}]$	DC motor back EMF constant
n	2	-	Gear ratio
K_t	0.317	$[\frac{Nm}{A}]$	Motor's torque constant

The experiment is purposed to obtain the absorption area for each controller designed in a specific equilibrium point and the answer to the question "how does a closer equilibrium point selection can affect transient and steady-state response".

Considering the origin as the first equilibrium point, the designed controller works properly and stabilizes the system while the output tracks its set-point. Results of a sample experiment is shown in (**Error! Reference source not found.**) where the initial state is as $x_{init} = \left[\frac{\pi}{15}, \frac{\pi}{30}, \frac{\pi}{30}, \frac{\pi}{30}, -\frac{\pi}{6}, \frac{\pi}{30}\right]^T$ and the set-point is $x_{ref} = \left[\pi, 0, \frac{\pi}{4}; 0; \frac{\pi}{4}; 0\right]^T$.

Now to determine the absorption area for the controller designed based on linearized system we increase the variable ψ in the set-point. Experiments shows that the designed controller is valid for all values assigned to ψ in the desired range, i.e. $-75\ to + 75\ [deg]$. Results of this part is shown in (**Error! Reference source not found.**) for $x_{ref} = \left[\pi, 0, \frac{\pi}{3}; 0; \frac{2\pi}{5}; 0\right]^T$. Simulation results indicate that the controller is valid in domain

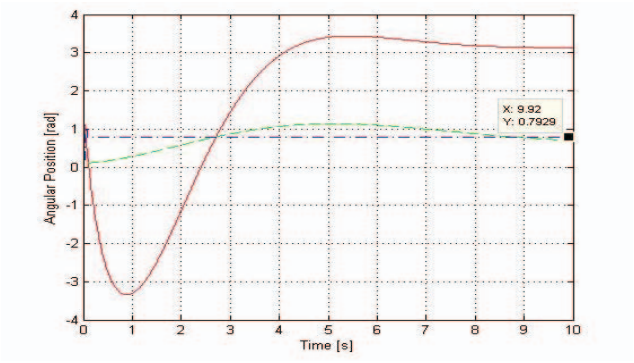

(a)

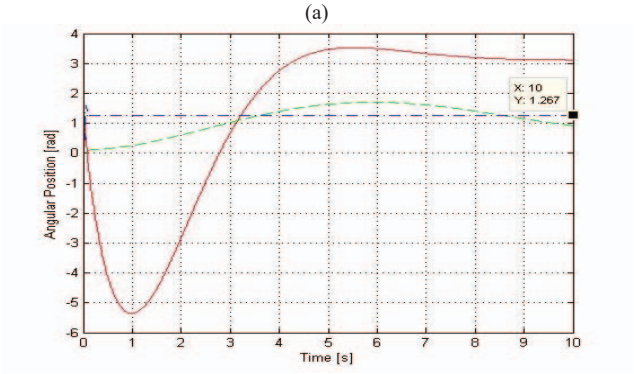

(b)

Fig. 7 The simulation results based on linearizing at the origin. Simple line (red) indicates θ while dashed line (green) represents ϕ and the doted line (blue) is showing the response for the variable ψ (a) Experiment 1: The system can track the desired values stably for desired $\psi = 45\ [deg]$. (b) Experiment 2: Despite the desired value is at maximum the controller is still valid for the model linearized at the origin.

of the robot's body pitch angle. Note that in this experiment the initial state is as the first experiment.

In the third experiment we are going to determine how a

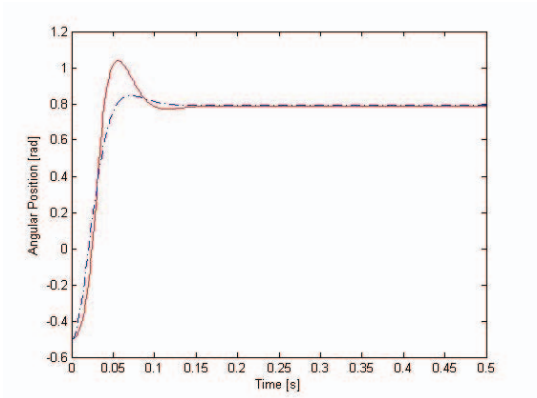

Fig. 6 Simulation results for first and third experiments. The Simple line indicates the response for the first experiment while dashed line represents the response for the third one.

closer equilibrium point selection can affects the System's transient response. To find out the answer we designed a controller based on linearizing the system around a new equilibrium point closer to the operating point, $x_{ss} = \left[\frac{4\pi}{5}, \frac{\pi}{30}, \frac{\pi}{6}, \frac{\pi}{30}, \frac{\pi}{6}, \frac{\pi}{30}\right]^T$ and choose the initial state as $x_{init} = \left[\frac{\pi}{15}, \frac{\pi}{30}, \frac{\pi}{30}, \frac{\pi}{30}, -\frac{\pi}{6}, \frac{\pi}{30}\right]^T$ and choose the set point like first experiment as $x_{ref} = \left[\pi, 0, \frac{\pi}{4}; 0; \frac{\pi}{4}; 0\right]^T$. Comparing the response for body pitch angle in this two different experiment, i.e. first and third experiment indicates that a linearizing at a closer point can considerably affect the transient response. Linearizing in a closer equilibrium, point can notably improve the systems damping speed and decrease the overshoot which is really important especially for the variable ψ base on physical limitations (Fig. 6). So it makes sense to design more than one controller in different equilibrium point in every updating step to obtain a better response.

IV. Conclusion and Future Work

In this paper we performed the modeling, analysis, and control of the tethered Segway on steep surfaces. The system has been simulated and its stability conditions have been shown. The result shows that the system can stably move on steep surfaces.

We plan to actually implement the proposed controller on our Dome Tethered Robot described in [3] and test the controller in action. Furthermore, a path planning for crossing over the dome surface is planned to be designed so that the robot can go autonomously to a desired point on a dome surface. In the future, we should consider the possible slippage of the wheels and design a robust controller to be able to control the robot in such conditions.

Acknowledgment

We like to thanks A. Nejadfard and H. Kebriaei for their feedback and help during the research. This project is partially funded and supported by Hosseinieh Ershad foundation and the Iranian National Science Foundation, grant number 91003683.

References

[1] A. Nejadfard, H. Moradi, and M. N. Ahmadabadi, "A multi-robot system for dome inspection and maintenance: Concept and stability analysis," in *2011 IEEE International Conference on Robotics and Biomimetics (ROBIO)*, 2011, pp. 853–858.

[2] K. Naderi, A. Nejadfard, H. Moradi, and M. N. Ahmadabadi, "A centralized potential field method for stable operation of a multi-robot dome inspection, repair, and maintenance system," in *2013 First RSI/ISM International Conference on Robotics and Mechatronics (ICRoM)*, 2013, pp. 96–101.

[3] M.H Salehpour, B. Zamanian, and H. Moradi, "The Design, Implementation, and Stability Analysis of a Human-Inspired Dome-Tethered Robot," in *2014 Second RSI/ISM International Conference on Robotics and Mechatronics (ICRoM)*, 2014

[4] M. Tavakoli, C. Viegas, L. Marques, J. Norberto, and A. T. de Almeida, "Magnetic omnidirectional wheels for climbing robots," in *2013 IEEE/RSJ International Conference on Intelligent Robots and Systems (IROS)*, 2013, pp. 266–271.

[5] O. Unver, A. Uneri, A. Aydemir, and M. Sitti, "Geckobot: a gecko inspired climbing robot using elastomer adhesives," in *Proceedings 2006 IEEE International Conference on Robotics and Automation, 2006. ICRA 2006*, 2006, pp. 2329–2335.

[6] Y. Yoshida and S. Ma, "Design of a wall-climbing robot with passive suction cups," in *2010 IEEE International Conference on Robotics and Biomimetics (ROBIO)*, 2010, pp. 1513–1518.

[7] Draz, M.U., M.S. Ali, M. Majeed, U. Ejaz, and U. Izhar. "Segway Electric Vehicle." In *2012 International Conference on Robotics and Artificial Intelligence (ICRAI)*, 34–39, 2012. doi:10.1109/ICRAI.2012.6413423.

[8] Khan, M.H., M. Chaudhry, T. Tariq, Q.-U.-A. Fatima, and U. Izhar. "Fabrication and Modelling of Segway." In *2014 IEEE International Conference on Mechatronics and Automation (ICMA)*, 280–85, 2014. doi:10.1109/ICMA.2014.6885709.

[9] Faizan, F., F. Farid, M. Rehan, S. Mughal, and M.T. Qadri. "Implementation of Discrete PID on Inverted Pendulum." In *2010 2nd International Conference on Education Technology and Computer (ICETC)*, 1:V1–48 – V1–51, 2010. doi:10.1109/ICETC.2010.5529304.

[10] Fabien, Brian. *Analytical System Dynamics: Modeling and Simulation*. Springer Science & Business Media, 2008.

[11] Bimbhra, P. S. Generalized Theory of Electrical Machines. Khanna, 2002.

[12] Albertos, Pedro, and Antonio Sala. *Multivariable Control Systems: An Engineering Approach*. 2004 edition. London: Springer, 2003.

[13] J.-J. E. Slotine and W. Li, Applied nonlinear control. Englewood Cliffs, N.J.: Prentice Hall, 1991.